Arch. Metall. Mater. **67** (2022), 4, 1299-1304

DOI: https://doi.org/10.24425/amm.2022.141055

MUHAMMAD RAZLAN ZAKARIA[1,2], HAZIZAN MD AKIL[3], MOHD FIRDAUS OMAR[1,2*], MOHD MUSTAFA AL BAKRI ABDULLAH[1,2], SHAYFULL ZAMREE ABD RAHIM[2], M. NABIAŁEK[4], J.J. WYSŁOCKI[4]

# HIERARCHICAL CARBON FIBER-CARBON NANOTUBES BY USING ELECTROSPRAY DEPOSITION METHOD WITH PRESERVED TENSILE PROPERTIES

In this study, the electrospray deposition (ESD) method was used to deposit carbon nanotubes (CNT) onto the surfaces of carbon fibers (CF) in order to produce hybrid carbon fiber-carbon nanotubes (CF-CNT) which is rarely reported in the past. Extreme high-resolution field emission scanning electron microscopy (XHR-FESEM), high-resolution transmission electron microscopy (HRTEM) and x-ray photoelectron spectroscopy (XPS) were used to analyse the hybrid carbon fiber-carbon nanotube (CF-CNT). The results demonstrated that CNT was successfully and homogenously distributed on the CF surface. Hybrid CF-CNT was then prepared and compared with CF without CNT deposition in terms of their tensile properties. Statistically, the tensile strength and the tensile modulus of the hybrid CF-CNT were increased by up to 3% and 25%, respectively, as compared to the CF without CNT deposition. The results indicated that the ESD method did not cause any reduction of tensile properties of hybrid CF-CNT. Based on this finding, it can be prominently identified some new and significant information of interest to researchers and industrialists working on CF based products.

*Keywords:* Hybrid materials; Carbon Nanotubes; Carbon Fiber

## 1. Introduction

Researchers have drawn significant attention to hierarchical or multiscale composites, where nanoscale materials are topologically combined with microscale reinforcements, provided that various synergistic results can be easily realised by utilising these materials [1]. Carbon nanotubes (CNT) are ideal candidates for nanoscale reinforcement due to their large surface area, good compatibility with polymers and excellent mechanical, electrical and thermal properties [2]. Meanwhile, carbon fibers (CF) have also received remarkable attention in micro scaling reinforcement due to their high stiffness, strength and lightness properties [3].

Hybridizing CF with CNT to enhance the interfacial properties of composites has been demanding topic for the last few decades [4-6]. Currently, several methods have been developed to hybridize CF with CNT, such as chemical vapour deposition (CVD) [7-10], electrophoretic deposition (EPD) [11-13] and chemical functionalization [14-16]. While all of these methods are commonly known to have successfully improving interfacial properties of polymer composites, but somehow, there are some drawbacks to each method especially in the reduction of tensile properties of hybrid CF-CNT [17]. In the case of the CVD method, the high processing temperature contributes to the reduction of the CF properties especially in the longitudinal direction [18,19]. Meanwhile for EPD and chemical functionalization, it has been reported that both methods expose CF and CNT to excessive chemical treatments, which can indirectly contribute to the reduction of the mechanical properties of CF and CNT [20-23].

Another emerging technique for the hybridization of the CF and CNT is the electrospray deposition (ESD) method [24]. This process is conducted at room temperature and the CF and CNT are not treated with excessive chemical treatments [25]. In addition, epoxy resin has been used as a binder to improve the adhesion between the CF and CNT [26]. Apart from that, there are other benefits offered by this technique such as cost effectiveness and the potential to manufacture on a large scale [27]. Until recently,

[1] UNIVERSITI MALAYSIA PERLIS, FACULTY OF CHEMICAL ENGINEERING TECHNOLOGY, KOMPLEKS PENGAJIAN JEJAWI 2, 02600 ARAU, PERLIS, MALAYSIA
[2] UNIVERSITI MALAYSIA PERLIS, GEOPOLYMER & GREEN TECHNOLOGY, CENTRE OF EXCELLENT (CEGEOGTECH PERLIS, MALAYSIA
[3] UNIVERSITI SAINS MALAYSIA, SCHOOL OF MATERIALS AND MINERAL RESOURCES ENGINEERING, ENGINEERING CAMPUS, 14300 NIBONG TEBAL, PULAU PINANG, MALAYSIA
[4] CZESTOCHOWA UNIVERSITY OF TECHNOLOGY, FACULTY OF PRODUCTION ENGINEERING AND MATERIALS TECHNOLOGY, DEPARTMENT OF PHYSICS 42-201 CZESTOCHOWA, POLAND

* Corresponding email: firdausomar@unimap.edu.my

the utilization of ESD in depositing CNT onto the surfaces of CF is still less reported due to its complexity of instrument set-up and therefore the knowledge is remains unclear.

Based on this limitation, this research is purposefully design to explore the effect of hybridization of the CF and CNT by using ESD method. The distribution of CNT on CF surface was characterized via extreme high-resolution field emission scanning electron microscopy (XHR-FESEM) and high-resolution transmission electron microscopy (HRTEM). Finally, the tensile properties of hybrid CF-CNT and CF without CNT deposition were evaluated and compared by single fiber tensile test.

## 2. Experimental

### 2.1. Materials

Multi-walled CNT with a length of 10-30 μm, an inner diameter of 5-10 nm, an outer diameter of 20-30 nm and a CF with a thickness of 0.3 mm were purchased from Sky Spring Nanomaterials Inc., Houston, TX, USA and Toray Industries Inc., Chuo-Ku, Tokyo, respectively. N-Methyl-2-pyrrolidone (NMP) solvent was purchased from Sigma-Aldrich, St. Louis, MO, USA. An epoxy adhesive (UV 367) that was rapidly cured in 3 seconds under UV light was purchased from Penchem Technologies Sdn. Bhd., Penang, Malaysia.

### 2.2. Preparation of hybrid CF-CNT

Hybrid CF-CNT was prepared using the electrospray deposition method. A sonicator (Q700, Qsonica, Melville, CT, USA) was used to disperse 0.1 g of CNT in 50 ml of NMP at a frequency of 50 kHz for 5 hours to prepare a CNT dispersion desirable for electrospray deposition. The sonicator was used to break down the agglomeration of the CNT and create a better distribution of the CNT. After that, 1 ml of UV 367 was applied to the CNT dispersion as a binder to improve the binding strength between the CNT and the CF. In preparation for electrospray deposition, the equipment consisted of a stainless steel needle (0.55 mm outer diameter, 0.3 mm inner diameter, 23G) and a steel plate as a ground electrode. The high voltage power supply precision (Model type ES20P-20W) is linked to the stainless steel needle and is capable of generating an applied voltage of 20 kV at resolution of 0.1 kV. The needle is fitted to a 20 ml syringe and the syringe is attached to a syringe pump (New Era Pump Systems, Inc., USA, Model NE-1600). This model of syringe pump was able to regulate flow rates of up to 0.001 μL/hr. CF was then mounted on the steel roller. Then, The CNT dispersion with a flow rate of 0.02 ml/min was then applied during the process with an applied voltage of 15 kV and a spray duration of 15 minutes. After completion of the spraying process, the CF was left to dry for 24 hours and the spraying process was repeated on the opposite side. Fig. 1 shows the setup of the electrospray deposition for this research.

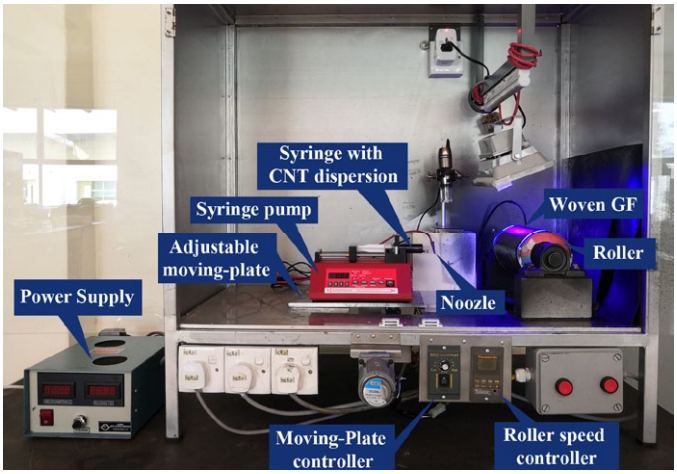


Fig. 1. General view of electrospray deposition process

### 2.3. Characterization of Hybrid CF-CNT

An extreme high-resolution field emission scanning electron microscope (XHR-FESEM) (Model: FEI Verios 460L) and a high-resolution transmission electron microscopy (HRTEM) (Model: Philip TECNAI 20) were used to observe the morphology of the CNT, CF and hybrid CF-CNT. X-ray photoelectron spectroscopy (XPS) was performed to investigate the elemental compositions on the surfaces of CNT, CF and hybrid CF-CNT. Wide scan spectra were obtain using the AXIS Ultra DLD, Kratos (UK) with an Al Ka X-ray source. The analysis was performed on an area of $300 \times 700$ μm$^2$ with the slot aperture and the pass energy of the hemispheric analyzer set at 60 eV for wide scan.

### 2.4. Single Fiber Test

Single fiber tensile test of CF and hybrid CF-CNT was performed using Diastron Lex810 miniature tensile (UK) in accordance to the ASTM C 1557 standard test method [28]. Prior to the test, a CF and hybrid CF-CNT were conditioned in a desiccator at room temperature for 24 hours. A single fiber tensile test was carried out using a 15 mm gage length and a 0.5 mm/min crosshead speed. Mitutoyo LSM 500S laser scan micrometer (Japan) with fiber dimensional analysis FDAS770 Diastron (UK) was used to measure the diameter of the single fiber. The diameters were determined across the single fiber at three different places and the average value was taken as the corresponding single fiber diameter. A total of 50 single fiber samples were measured for each sample.

## 3. Results and discussion

The surface morphologies of the CNT, CF and hybrid CF-CNT were characterized by using SEM. Fig. 2a-b shows the SEM images of the CNT with diameter about 10-20 nm. Fig. 2c-d displays the morphological structure of the CF with

diameter about 6-8 μm. Based on the figures, it can be clearly seen the smooth surface of CF with grooves running along the longitudinal direction before deposition of CNT. The Fig. 2e-f shows the FESEM images of the hybrid CF-CNT. It was observed that the CNT was homogeneously distributed and covered the entire surface of the CF. More interestingly, the ESD method succeeded in properly depositing the CNT on the CF surface without forming any agglomeration. This phenomenon was due to the use of high-electric fields to convert the CNT suspension into nanodroplets with a uniform coating.

HRTEM provides detailed analysis of carbon microstructure in the CNT, CF and hybrid CF-CNT specimen. Fig. 3 shows HR-TEM images of the CNT, CF and hybrid CF-CNT. Fig. 3a shows the HRTEM images of the CNT, which illustrated that CNT is multi-walled carbon nanotube (MWCNT). From the HRTEM images of Fig. 3b, the graphitic structure of the CF is tortuosity and not well oriented as compared to graphitic structure of CNT. This may be due to the presence of disorder or amorphous carbon. Fig. 3c shows the HRTEM images of hybrid CF-CNT. From the images, it can be observed the CNT was attached on

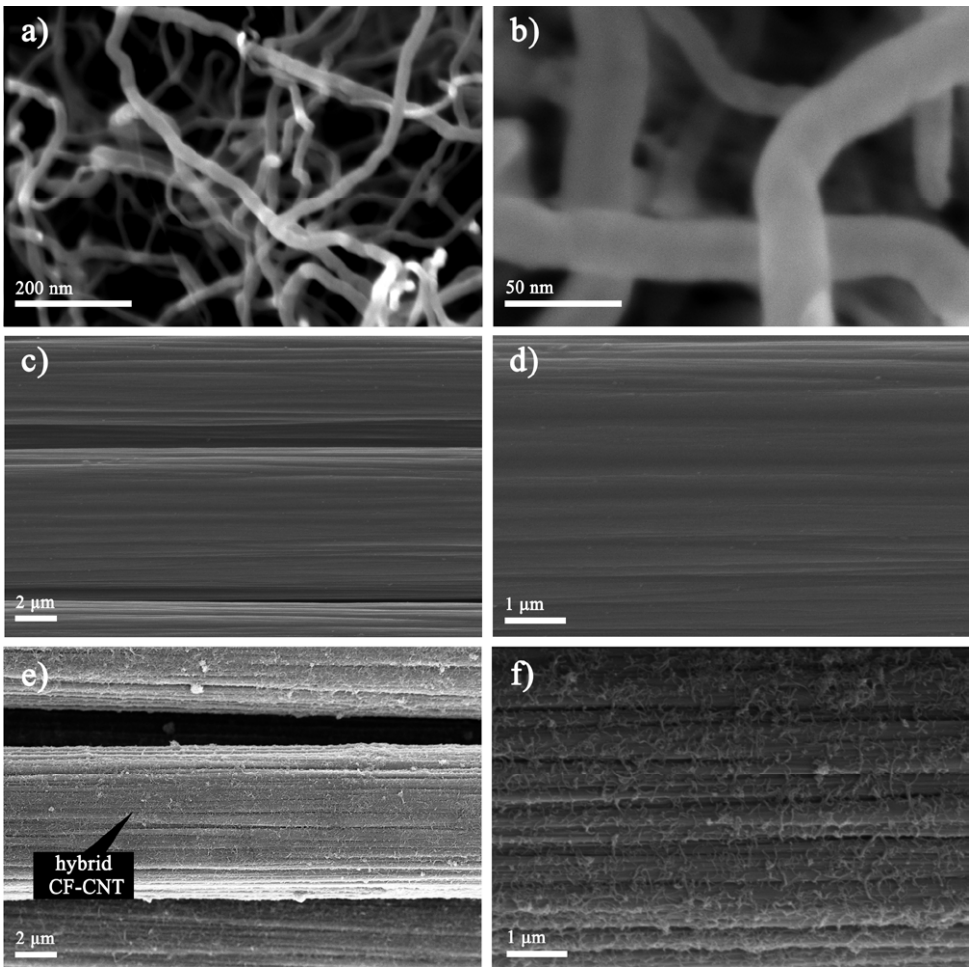


Fig. 2. SEM images of (a-b) CNT, (c-d) CF and (e-f) Hybrid CF-CNT

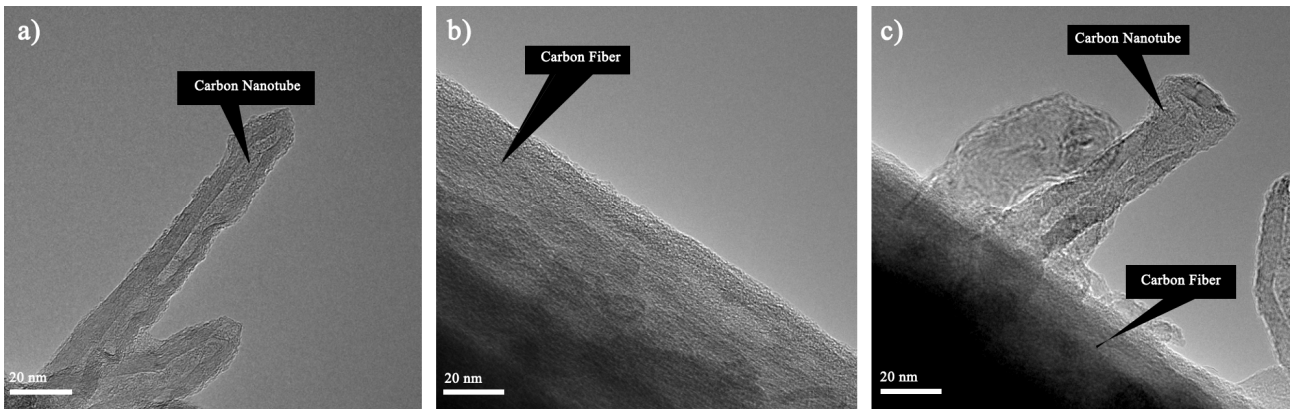


Fig. 3. HRTEM images of (a) CF, (b) CNT and (c) Hybrid CF-CNT

the CF surface, which indicated that the CNT was successfully deposited on the CF surface via ESD method. In addition, the CNT is preserved in the form of a tubular structure without significant damage to the CNT wall and retain similar to the HRTEM image of the CNT in Fig. 3a. It can be also seen from the HRTEM image that the structure of CF after the deposition of CNT is preserved from any damage caused by the high-electric fields of ESD method. Similar findings have been reported by Li et al. [24] where they also agreed that ESD method does not cause any significant damage to the structure of the CF and CNT and therefore, indirectly contributed to the better tensile performances than that of other hybridization methods. Moreover, the ESD method can also distribute CNT on the CF surface without any form of agglomeration.

As is well known, the XPS is a very useful instrument for determining chemical composition and functional groups of CNT and CF. Fig. 4 shows the XPS wide-scan spectrum of CNT, CF and hybrid CF-CNT. Based on the result, the CNT, CF and hybrid CF-CNT show a strong C1s peak at a binding energy of 284.4 eV, 284.6 eV and 284.6 eV, respectively. These peaks designate to the C-C bond from the graphitic structure of the CNT and CF. The CNT shows higher C1s peak compared to CF. This indicated the CNT has more C-C bonds from $sp^2$ carbon atom of graphite structure. Besides, the CNT, CF and hybrid CF-CNT also show a presence of O1s peak at a binding energy of 533.3 eV, 533.0 eV and 533.0 eV, respectively. The presence of these peaks designates to the C-O bond. From the observation, it can be seen the CF shows high O1s peak compared to the CNT. The C/O ratio of the CNT, CF and hybrid CF-CNT were calculated and summarized in TABLE 1. From the result, the CNT shows the highest C/O ratio. This indicates the CNT has high graphitic structure. Based on the C/O ratio of hybrid CF-CNT, it can be observed that deposition of CNT has increased the C/O ratio of CF. As discussed previously, C1s spectrum of XPS are influenced by the graphite structure of CNT and CF. Based on the result, the CNT shows a higher peak at the C1s spectrum as compared to the CF. In addition, the peak of CF at the C1s spectrum and C=C stretching show increases in intensity after deposition of CNT, indicated that the CNT was successfully deposited on the surface of CF.

TABLE 1

Mass percentages and C/O ratio obtained by XPS on CNT, CF and hybrid CF-CNT

| Sample | C (%) | O (%) | C/O ratio |
|---|---|---|---|
| CNT | 95.36 | 4.64 | 20.55 |
| CF | 78.00 | 22.00 | 3.56 |
| Hybrid CF-CNT | 87.72 | 12.28 | 7.14 |

The single fiber test was performed in order to evaluate the tensile properties of hybrid CF-CNT and to study whether the ESD process does give any collateral effect to their tensile properties. Tensile stress-strain curves of CF and hybrid CF-CNT are shown in Fig. 5. Meanwhile, TABLE 2 summarized the tensile strength and tensile modulus of CF and hybrid CF-CNT. The result showed that the tensile strength of hybrid CF-CNT was 4517 MPa, which is 3% higher than that of CF without deposited CNT (4382 MPa). Meanwhile, the tensile modulus of hybrid CF-CNT increased up to 412 GPa, which is about 25% higher as compared to CF. Based on the recorded result, it was experimentally proven that the ESD process did not cause any significant reduction of tensile properties of hybrid CF-CNT as compared to the other methods.

More interestingly, this method could also improve the tensile strength and the tensile modulus of hybrid CF-CNT by modifying and improving the surface flaws of CF during manufacturing. Besides that, the UV cured epoxy which was used as a binder to attach CNT on the CF surface could also retard the potential flaws on the CF surface. This argument was in agreement with the one that has been reported by Li et al. [24].

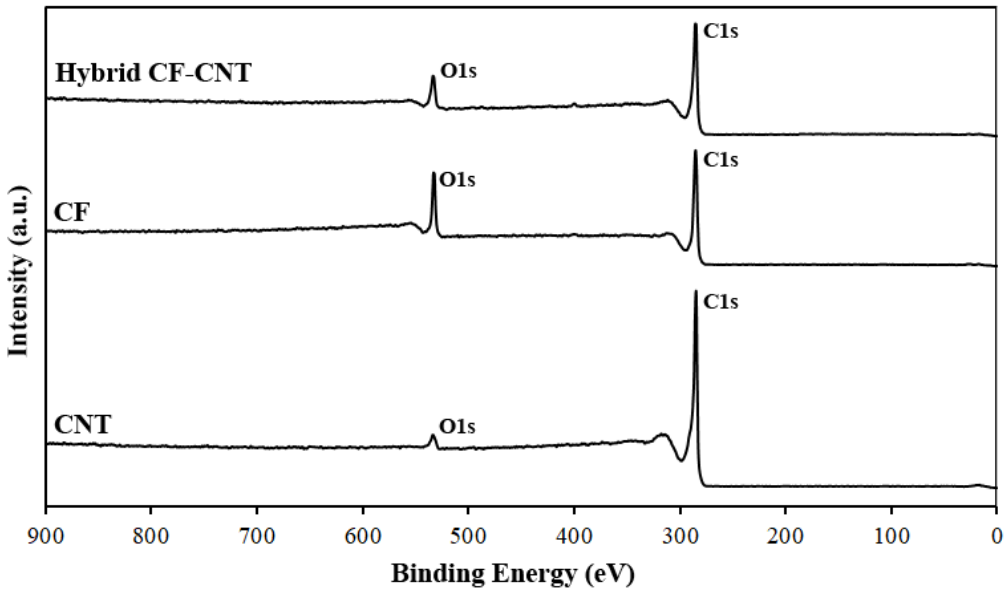


Fig. 4. XPS wide-scan spectrum of CNT, CF and hybrid CF-CNT

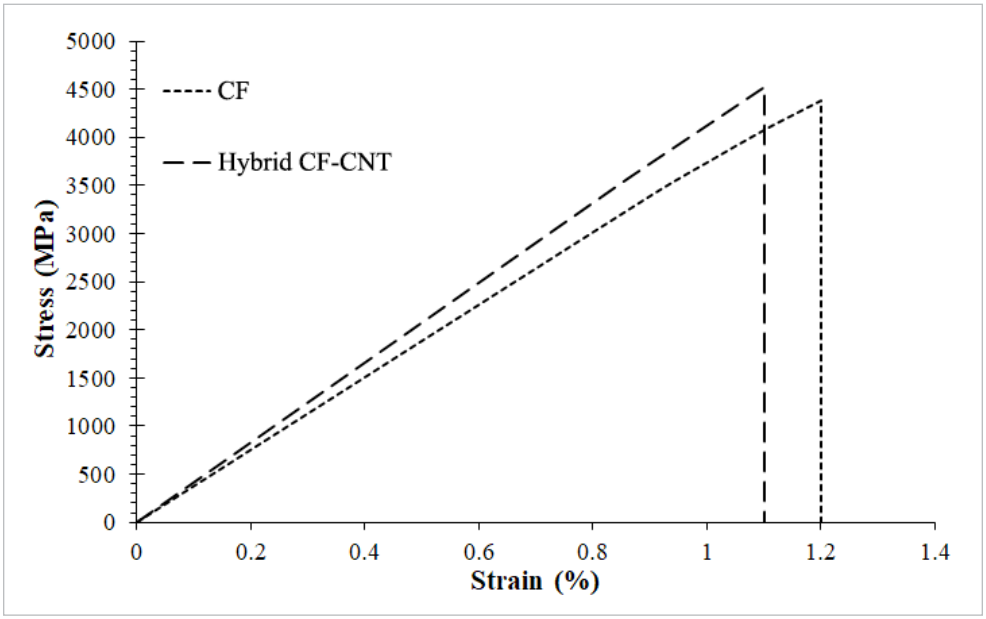


Fig. 5. Tensile stress-strain curves of CF and hybrid CF-CNT

Generally, the tensile properties of hybrid CF-CNT produced via CVD and chemical functionalization have recorded the decreasing pattern in both tensile strength and tensile modulus [29,30]. This reduction may be attributed to the high processing temperature of CVD and permanent exposure of CF and CNT under strong acid treatment during chemical functionalization. Qian and his co-workers were also recorded losses in the tensile strength and tensile modulus of around 17% and 2%, specifically for the hybrid CF-CNT produced by using the CVD method [31]. As for the chemical functionalization method, Zhang et al. had reported a decrease of 3% in the tensile strength of the hybrid CF-CNT [32].

TABLE 2

Tensile properties of CF and Hybrid CF-CNT

| Samples | Tensile strength (MPa) | Tensile Modulus (GPa) |
|---|---|---|
| CF | 4382 ± 48 | 351 ± 18 |
| Hybrid CF-CNT | 4517 ± 54 | 412 ± 23 |

## 4. Conclusion

Hybrid CF-CNT specimens have been successfully prepared using ESD method with an applied voltage of 15 kV and a spray duration of 15 minutes. This method used high-electric field to produce a uniform coating and homogeneous distribution of CNT on the CF surface. The XHR-FESEM, HRTEM and XPS results proved that the ESD method had homogenously deposited CNT on the CF surface. Interestingly, the hybrid CF-CNT specimens had also showed higher tensile properties as compared to the CF without CNT deposition. From these findings, it can be concluded that the ESD method is reliable and ready for future prospect of hybrid materials processing.

**Acknowledgement**

The authors would like to acknowledge Universiti Sains Malaysia (USM) RUI 1001/PBAHAN/8014047 for sponsoring and providing financial assistance during this research work and Universiti Malaysia Perlis for sponsoring postdoctoral fellowship.

## REFERENCES

[1] S. Zhang, L. Gao, J. Han, Z. Li, G. Zu, X. Ran, Y. Sun, Composites Part B: Engineering **165**, 183-192 (2019).

[2] M.R. Zakaria, M.H. Abdul Kudus, H. Md. Akil, M.Z. Mohd Thirmizir, Composites Part B: Engineering **119**, 57-66 (2017).

[3] N. Nosbi, H.F. Ahmad Marzuki, M.R. Zakaria, W.F. Wan Ali, F. Javed, M. Ibrar, Processes **8** (11), (2020).

[4] N. Forintos, T. Czigany, Composites Part B: Engineering **162**, 331-343 (2019).

[5] M. Fontana, R. Ramos, A. Morin, J. Dijon, Carbon **172,** 762-771 (2021).

[6] Y. Wu, X. Cheng, S. Chen, B. Qu, R. Wang, D. Zhuo, L. Wu, Materials & Design **202**, 109535 (2021).

[7] A.Y. Boroujeni, M. Al-Haik, Composites Part B: Engineering **164**, 537-545 (2019).

[8] H.S. Bedi, M. Tiwari, P.K. Agnihotri, Carbon **132**, 181-190 (2018).

[9] M. Russello, E.K. Diamanti, G. Catalanotti, F. Ohlsson, S.C. Hawkins, B.G. Falzon, Composite Structures **206**, 272-278 (2018).

[10] Z. Ma, Y. Wang, J. Qin, Z. Yao, X. Cui, B. Cui, Y. Yue, Y. Wang, C. Wang, Ceramics International **47** (2), 1625-1631 (2021).

[11] J. Ma, X. Lan, B. Niu, D. Fan, Materials Chemistry and Physics **192**, 210-214 (2017).

[12] X. Yao, X. Gao, J. Jiang, C. Xu, C. Deng, J. Wang, Composites Part B: Engineering **132**, 170-177 (2018).

[13] Q. Shen, H. Li, W. Li, Q. Song, Journal of Alloys and Compounds **738**, 49-55 (2018).
[14] W. Zhang, X. Deng, G. Sui, X. Yang, Carbon **145**, 629-639 (2019).
[15] H. Cui, Z. Jin, D. Zheng, W. Tang, Y. Li, Y. Yun, T.Y. Lo, F. Xing, Construction and Building Materials **181**, 713-720 (2018).
[16] W. Shen, R. Ma, A. Du, X. Cao, H. Hu, Z. Wu, X. Zhao, Y. Fan, X. Cao, Applied Surface Science **447**, 894-901 (2018).
[17] M.R. Zakaria, H. Md Akil, M.H. Abdul Kudus, F. Ullah, F. Javed, N. Nosbi, Composites Part B: Engineering **176,** 107313 (2019).
[18] F. An, C. Lu, J. Guo, S. He, H. Lu, Y. Yang, Applied Surface Science **258** (3), 1069-1076 (2011).
[19] H. Qian, A. Bismarck, E.S. Greenhalgh, G. Kalinka, M.S.P. Shaffer, Chemistry of Materials **20** (5), 1862-1869 (2008).
[20] K.L. Kepple, G.P. Sanborn, P.A. Lacasse, K.M. Gruenberg, W.J. Ready, Carbon **46** (15), 2026-2033 (2008).
[21] Q. An, A.N. Rider, E.T. Thostenson, Carbon **50** (11), 4130-4143 (2012).
[22] H. Yao, X. Sui, Z. Zhao, Z. Xu, L. Chen, H. Deng, Y. Liu, X. Qian, Applied Surface Science **347**, 583-590 (2015).
[23] J. Qin, C. Wang, Y. Wang, S. Su, Z. Yao, Z. Ma, Q. Gao, M. Yu, Q. Wang, H. Wei, Polymer Testing **93**, 106892 (2021).
[24] Q. Li, J.S. Church, M. Naebe, B.L. Fox, Carbon **109**, 74-86 (2016).
[25] M.R. Zakaria, H. Md Akil, M.F. Omar, M.H. Abdul Kudus, F.N.A. Mohd Sabri, M.M.A.B. Abdullah, Composites Part C: Open Access **3**, 100075 (2020).
[26] M.R. Zakaria, H.M. Akil, M.F. Omar, M.M.A.B. Abdullah, A.A.A. Rahman, M.B.H. Othman, Nanotechnology Reviews **9** (1), 1170-1182 (2020).
[27] Q. Li, J.S. Church, M. Naebe, B.L. Fox, Composites Part A: Applied Science and Manufacturing **90**, 174-185 (2016).
[28] ASTM C1557-20, Standard Test Method for Tensile Strength and Young's Modulus of Fibers, ASTM International, West Conshohocken, PA, 2020, www.astm.org
[29] H. Qian, A. Bismarck, E.S. Greenhalgh, M.S. Shaffer, Composites Part A: Applied science and manufacturing **41** (9), 1107-1114 (2010).
[30] R. Zhang, C. Wang, L. Liu, H. Cui, B. Gao, Applied Surface Science **353**, 224-231 (2015).
[31] H. Qian, A. Bismarck, E.S. Greenhalgh, M.S.P. Shaffer, Composites Part A: Applied Science and Manufacturing **41** (9), 1107-1114 (2010).
[32] R.L. Zhang, C.G. Wang, L. Liu, H.Z. Cui, B. Gao, Applied Surface Science **353**, 224-231 (2015).